

Detecting and Attributing Episodic High Background Ozone Events

by **Arlene M. Fiore**,
R. Bradley Pierce,
Russell R. Dickerson,
and **Meiyun Lin**

Arlene M. Fiore is with the Department of Earth and Environmental Sciences and Lamont-Doherty Earth Observatory of Columbia University, Palisades, NY; **R. Bradley Pierce** is with the NOAA/NESDIS, Center for Satellite Applications and Research (STAR), Advanced Satellite Products Branch (ASPB), Madison, WI; **Russell R. Dickerson** is with the Department of Atmospheric and Oceanic Science, University of Maryland, College Park, MD; and **Meiyun Lin** is with the Department of Atmospheric and Oceanic Sciences, Princeton University, Princeton, NJ. E-mail: Arlene M. Fiore amfiore@ldeo.columbia.edu.

Disclaimer: The views, opinions, and findings contained in this report are those of the authors and should not be construed as an official National Oceanic and Atmospheric Administration or U.S. Government position, policy, or decision.

A summary of recent work by AQAST members that combines satellite products, in situ measurements, and models to detect and attribute observed episodic high-ozone events to three specific background sources: wildfires, stratospheric intrusions, and Asian pollution.

The present formulation of the National Ambient Air Quality Standard (NAAQS) for ozone (O₃) considers the fourth highest daily maximum 8-hour average concentration to determine attainment status within specific areas. In order to achieve compliance with the 8-hour O₃ NAAQS, the three-year average of this statistic must not exceed the designated level, currently 75 parts per billion (ppb). The U.S. Clean Air Act Section 319 (b)(3)(B), however, recognizes that events can episodically exceed thresholds for O₃ and other NAAQS due to influences beyond the control of domestic air agencies. Such “exceptional events” can be exempted from counting toward regulatory decisions, such as non-attainment determinations, if air agencies can demonstrate that specific components of background O₃ led to the observed exceedance (see sidebar, “What Are Background Ozone and Exceptional Events?” on page 25). The origin of individual high O₃ events thus needs to be understood and contributions from individual sources quantified. This attribution to specific sources becomes increasingly important as the O₃ NAAQS is tightened (i.e., the threshold lowered), as has been proposed on the basis of health evidence.¹

Ozone source attribution is confounded by a lack of coincident measurements of related species (e.g., water vapor, carbon monoxide) at sufficient spatial resolution that could enable an unambiguous attribution from observations. Many background events, however, are associated with broad, synoptic-scale features evident from satellite products and resolved in models. Following are examples from recent work by AQAST members that combines satellite products, in situ measurements, and models to detect and attribute observed episodic high O₃ events to three specific background sources: wildfires, stratospheric intrusions, and Asian pollu-

tion. While the ground-based and space-based measurements are usually provided on a daily basis, the in situ aircraft and sonde measurements in the examples below are generally not routinely available.

Wildfires

In early July 2002, lightning sparked several fires in central Quebec that consumed approximately 2.5×10^9 m² of forest. A massive smoke plume, visible from space (see Figure 1) was swept by the meteorological conditions to the heavily populated areas of the U.S. East Coast.² Coincident with the arrival of the smoke was an air pollution event in which ambient monitors in Maryland exceeded the O₃ NAAQS. Was the fire to blame?

Fires generate aerosols and O₃ precursor gases such as carbon monoxide (CO) and volatile organic compounds (VOCs), but not necessarily nitrogen oxides (NO_x) needed alongside the VOCs to produce O₃, and thus, do not always lead to substantial O₃ production.³ Measurements from aircraft (see Figure 2) revealed a peak ozone mixing ratio over Maryland of nearly 160 ppb, more than twice the current 75-ppb ozone NAAQS threshold, coinciding with enhanced fire effluents (aerosols and CO), but not U.S. anthropogenic emissions (e.g., sulfur dioxide).

These in situ measurements, combined with numerical simulation and lidar records, demonstrated that the O₃ pollution layer generated by the fires mixed down to the surface, leading to the observed ground-level O₃ above the NAAQS. A similar approach can be used to identify high fine particulate matter (PM_{2.5}) events resulting from wildfires. On the basis of this integrated analysis of in situ measurements, satellite products, and model data, the Maryland Department of the Environment

Figure 1. MODIS (Moderate Resolution Imaging Spectrometer) visible image (July 7, 2002) of the smoke plume that was advected from Quebec (under the influence of a low pressure system over the Maritime provinces) and fanned out over the U.S. East Coast. Red dots indicate the locations of active fires.^{2a}

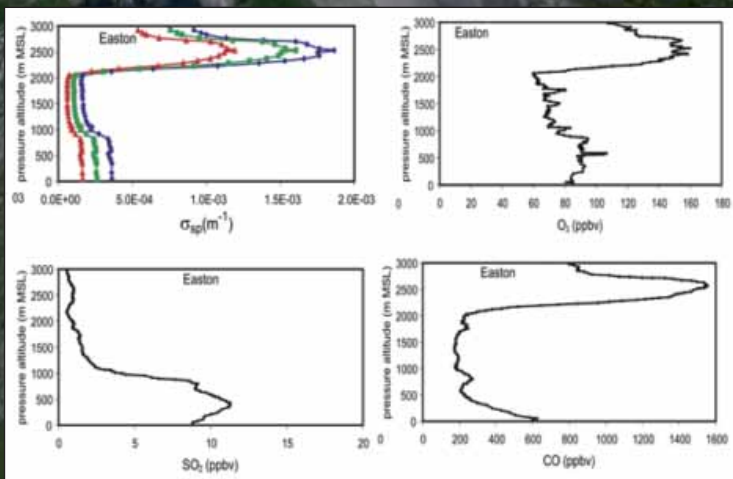
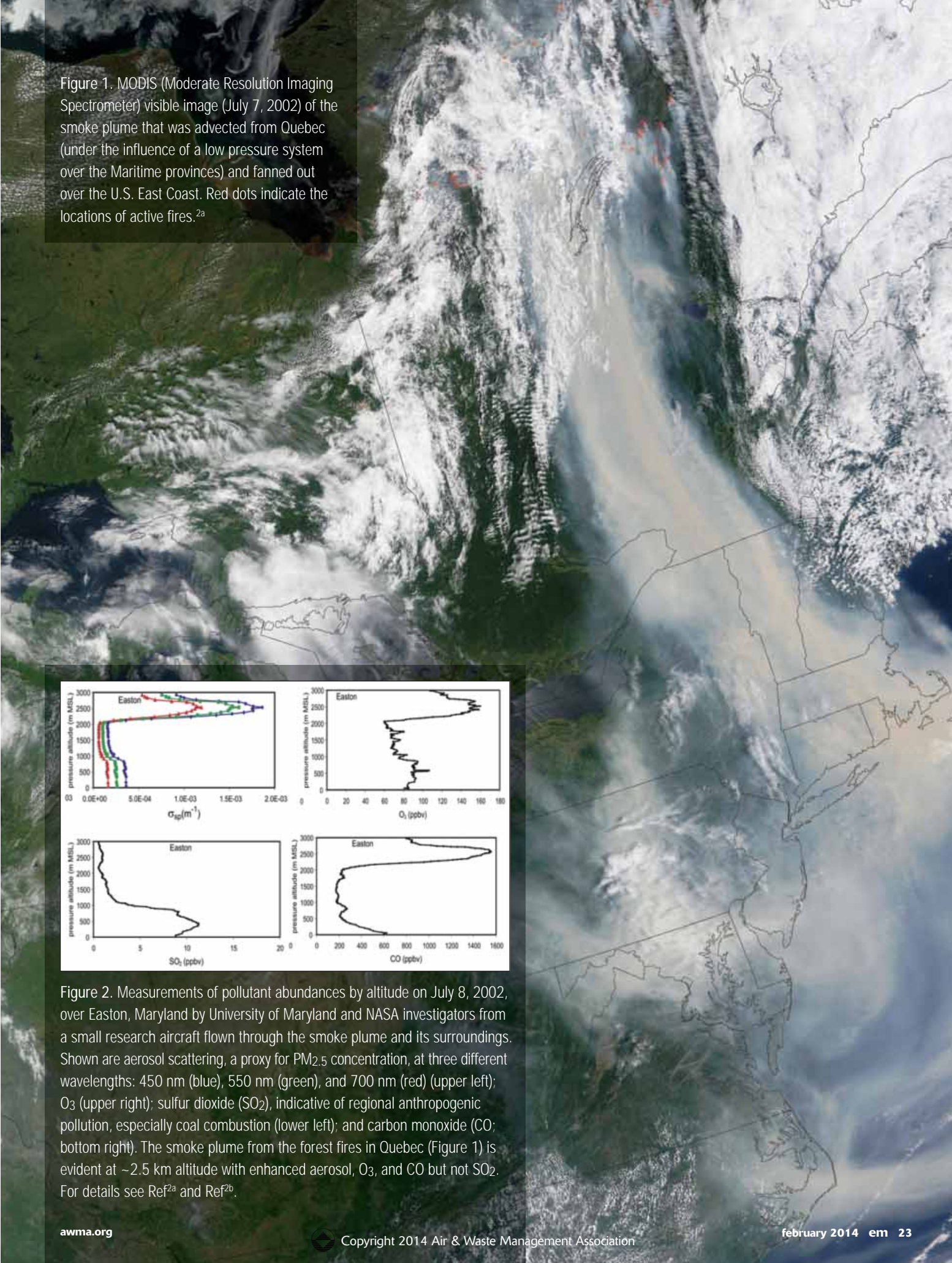
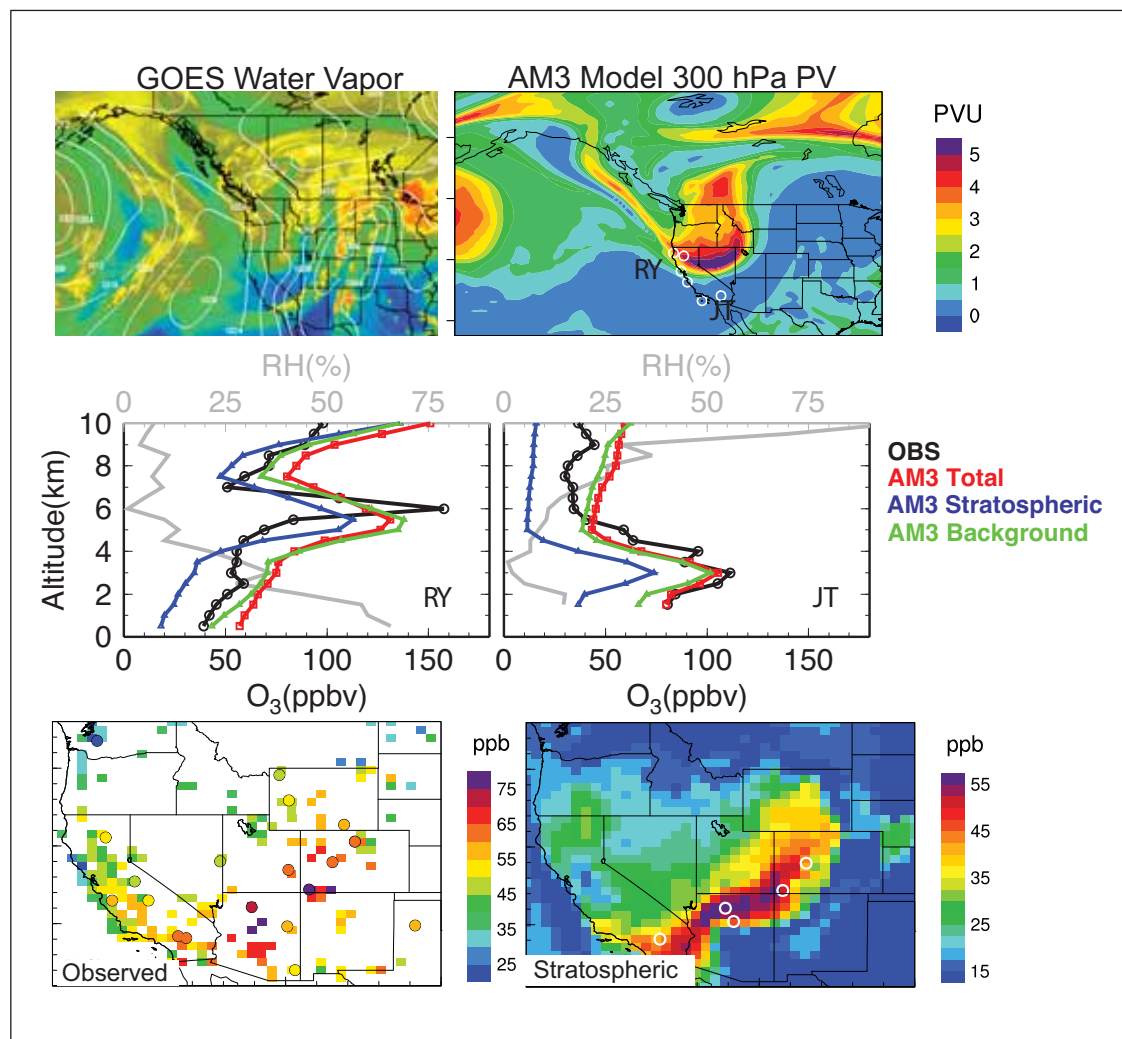


Figure 2. Measurements of pollutant abundances by altitude on July 8, 2002, over Easton, Maryland by University of Maryland and NASA investigators from a small research aircraft flown through the smoke plume and its surroundings. Shown are aerosol scattering, a proxy for $PM_{2.5}$ concentration, at three different wavelengths: 450 nm (blue), 550 nm (green), and 700 nm (red) (upper left); O_3 (upper right); sulfur dioxide (SO_2), indicative of regional anthropogenic pollution, especially coal combustion (lower left); and carbon monoxide (CO; bottom right). The smoke plume from the forest fires in Quebec (Figure 1) is evident at ~2.5 km altitude with enhanced aerosol, O_3 , and CO but not SO_2 . For details see Ref^{2a} and Ref^{2b}.

Figure 3. Example of integrating satellite, in situ, and model data to demonstrate the role of a stratospheric intrusion in enhancing surface O₃ over the western United States.

The GOES water vapor images show dry air in the mid-to-upper troposphere (blue colors in upper left; contours show sea level pressure) on May 28, 2010, coincident with a tongue of enhanced potential vorticity (PV), a dynamical marker for stratospheric air, simulated by the AM3 model (upper right). O₃ measured by balloon sondes on May 28, 2010 (black line in middle panels), launched at the locations indicated in the upper right panel, show an enhanced O₃ layer at ~6km in northern California (Point Reyes; RY) and another in the lower troposphere (~3 km) in southern California (Joshua Tree; JT) associated with dry air (grey line, relative humidity). The AM3 model (red line) attributes this high O₃ layer to North American Background (NAB) O₃ (green line), predominantly due to stratospheric influence (blue line; using approach described in Ref⁴). Ground-based monitors record a surface O₃ enhancement on May 29, 2010, extending southwest-northeast over Arizona and Colorado (bottom left) in the same region where the AM3 model simulates elevated stratospheric O₃ levels (bottom right). Adapted from Ref⁴.



requested, and the U.S. Environmental Protection Agency (EPA) granted, “exceptional event” status during this episode for both O₃ and PM_{2.5}.

Stratospheric Intrusions

Thirteen stratospheric intrusions were found to contribute to raising western U.S. surface O₃ levels during April through June of 2010 (see Table 1).⁴ Figure 3 shows one of these events, diagnosed using the GFDL AM3 model⁵ and a suite of observations. On May 28, 2010, space-based observations of upper tropospheric water vapor show dry air where the GFDL AM3 model simulates high potential vorticity (PV; a marker for stratospheric air). The model and balloon sonde measurements show layers with enhanced O₃ descending in altitude southward along the coast of California. These enhancements are attributed by the model to stratospheric influence, consistent with measured dry air (low relative humidity).

A model simulation of North American Background (NAB) O₃ (see sidebar) indicates that the observed enhancements are not mainly associated with domestic O₃ pollution. The following day (May 29, 2010), the model indicates a surface influence from stratospheric O₃ coincident with observed regional surface O₃ enhancements. In light of events such as those demonstrated in Figure 3, EPA recently formed a stratospheric O₃ intrusion (SI) working group consisting of federal government scientists and air quality managers, with input from state and local agencies and academia. One of their foci is to provide satellite-based support for SI forecasting and related exceptional event analysis.

The Infusing satellite Data into Environmental Applications – International (IDEA-I; http://cimss.ssec.wisc.edu/imapp/ideai_v1.0.shtml) software package is being adapted to provide satellite based

SI forecasting capabilities. IDEA-I is an open source, globally configurable version of Infusing satellite Data into Environmental air quality Applications (IDEA)⁶ that provides a satellite-based aerosol forecasting, visualization, and data synthesis tool. An expansion of IDEA-I includes SI trajectory forecasts initialized using real-time, space-based measurements of O₃, temperature, and water vapor to identify signatures of stratospheric air (dry air with high O₃) within the troposphere. IDEA-I SI

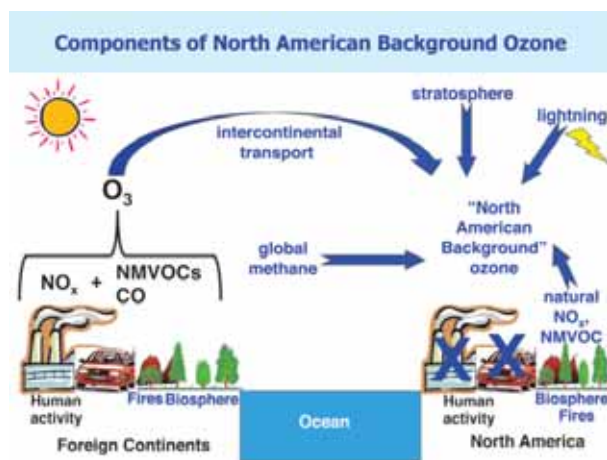
forecasts use measurements from several instruments aboard satellites: the Atmospheric Infrared Sounder (AIRS), the Infrared Atmospheric Sounding Interferometer (IASI), and the Cross-track Infrared Sounder (CrIS; http://cimss.ssec.wisc.edu/cssp/uwhsrvtv_edr_v1.2.shtml). When potential SI profiles are identified (based on three criteria: pressures below 500 hPa, O₃ above 80 ppb and dew point depressions of more than -15 °C), forward trajectories are initialized and used to predict

► What Are Background Ozone and Exceptional Events?

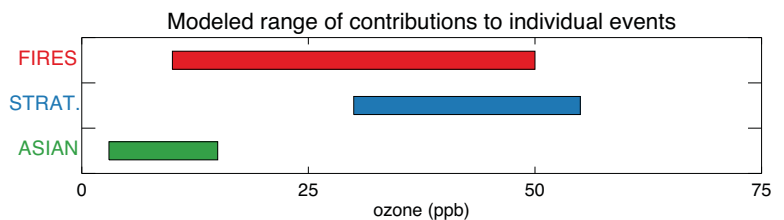
North American Background (NAB) O₃ is the concentration of O₃ in surface air that would occur in the absence of North American anthropogenic emissions.¹¹ NAB O₃ thus includes O₃ produced from natural nitrogen oxides (NO_x) and non-methane volatile organic compound (NMVOC) precursors, from foreign anthropogenic precursors, from global methane (including U.S. methane emissions which are not regulated), and transported from the stratosphere (see schematic). By definition, estimating background relies on models.

Ozone concentrations measured at remote sites, termed “baseline O₃” by a recent National Research Council report,¹² provide important constraints on model NAB estimates. NAB O₃ levels vary with altitude, season, and synoptic conditions, with the highest levels generally occurring over the high-altitude western United States during spring.¹³ The figure below shows model-based ranges for maximum episodic contributions from fires,¹⁴ stratospheric intrusions,⁴ and Asian pollution^{10,15} to high O₃ events in U.S. surface air. These model estimates motivate a need for accurate observational constraints to attribute unambiguously observed high O₃ events to sources other than North American anthropogenic emissions.

Such attribution could qualify the event for “exceptional event” status under the U.S. Clean Air Act. An exceptional event is a NAAQS exceedance that would not have occurred but for the influence of sources beyond the control of U.S. air agencies, and can be exempted from the dataset used for regulatory determinations, such as classifying a region as non-attainment.



Sources of North American Background (NAB) O₃ (blue labels and arrows). The blue Xs over North American human activities leading to O₃ precursor emissions indicate that those sources are not included in the definition of NAB O₃.



Range of contributions from components of North American Background (NAB) O₃ estimated with regional or global atmospheric chemistry models to individual high O₃ episodes in surface air. Shown are estimates for wildfires (FIRES),¹⁴ stratospheric intrusions (STRAT.),⁴ and Asian pollution (ASIAN).^{10, 15} These components add to local and regional pollution, and can contribute to total surface ozone exceeding the current 75 ppb threshold for the U.S. O₃ NAAQS.

Table 1. Stratospheric ozone intrusion events over the western United States from April–June 2010, adapted from Reference 4.⁴ The event shown in Figure 3 is highlighted in bold.

Event Date(s)	Major surface impact regions	Peak daily maximum 8-hr average O ₃	Number of exceedances at ground sites	Type of observations used to detect the intrusion
Apr. 7	Colorado, New Mexico	71	-	satellite
Apr. 9	Wyoming	75	1	satellite
Apr. 12–15	Four Corners Region	86	13	satellite
Apr. 21–23	Colorado, New Mexico	72	-	satellite
Apr. 28–29	Colorado, Wyoming	69	-	satellite
May 11–13	Arizona, New Mexico, W. Texas	74	-	satellite, lidar, ozonesondes,
May 18–21	Wyoming	74	-	satellite, ozonesondes
May 22–24	Colorado, New Mexico	79	4	satellite, lidar, ozonesondes
May 27–29	Arizona, California, Colorado	82	5	satellite, ozonesondes
Jun. 7–8	Idaho, Utah, Wyoming	76	3	satellite, ozonesondes
Jun. 9–14	California, Utah, Spread in Southwest	73	-	satellite, ozonesondes
Jun. 16–17	Colorado	67	-	satellite, ozonesondes
Jun. 22–23	Colorado	77	1	satellite

whether these stratospheric air masses are likely to impact the surface over the next 48 hours.

Figure 4 illustrates the IDEA-I SI trajectory forecasts along with model simulations and in situ measurements. These images provide corroborating evidence to demonstrate that a deep stratospheric intrusion led to a surface O₃ event above the NAAQS threshold. Figure 4a shows an IDEA-I SI forecast indicating downward transport of high O₃ air over northeastern Wyoming and Montana on June 6, 2012, when the Thunder Basin monitor in northeastern Wyoming reached 100 ppb at local noon. Enhanced O₃ (above 80 ppb) and PV (above 1.5 PVU) over central California on June 5, 2012, from the Real-time Air Quality Modeling System (RAQMS)⁷ indicates stratospheric air extending down into the troposphere along the northern flank of a relatively strong (45 ms⁻¹) jet at 120°W (see Figure 4b). Elevated O₃ levels were also measured by the NASA Ames AJAX project as the aircraft⁸ intersected the analyzed SI event (see Figure 4c). This analysis is included in a submitted exceptional event demonstration package (by Wyoming Department of Environmental Quality/Air Quality Division to EPA; <http://deq.state.wy.us/>

[aqd/ExceptionalEvents/June_6_2012ThunderBasin/June_6_2012_SI_Package.pdf](http://deq.state.wy.us/aqd/ExceptionalEvents/June_6_2012ThunderBasin/June_6_2012_SI_Package.pdf)).

Asian Pollution

A comprehensive review of Asian pollution impacts on North American surface O₃ was recently published.⁹ Figure 5 demonstrates a new approach to identifying days with the highest potential for importing Asian pollution into western United States surface air.¹⁰ Daily CO columns from the AIRS instrument aboard the Aqua satellite are correlated with a time series of Asian O₃ pollution estimated with the GFDL AM3 model, sampled at Grand Canyon National Park, Arizona, and lagged by two days. The region over the eastern North Pacific Ocean with higher correlations implies that the AIRS CO columns are generally enhanced there two days before the model simulates Asian pollution reaching Grand Canyon National Park. While the correlations are not sufficiently strong to use directly as a predictor, they imply there is useful information in the space-based observations. The region identified here could be used to initialize the IDEA-I model (as for the stratospheric intrusion application) and forecast Asian pollution plumes reaching U.S. surface air.

Figure 4. Example analysis used to document a stratospheric intrusion that led to a high-ozone event in excess of the U.S. NAAQS threshold and included in an exceptional event demonstration package.

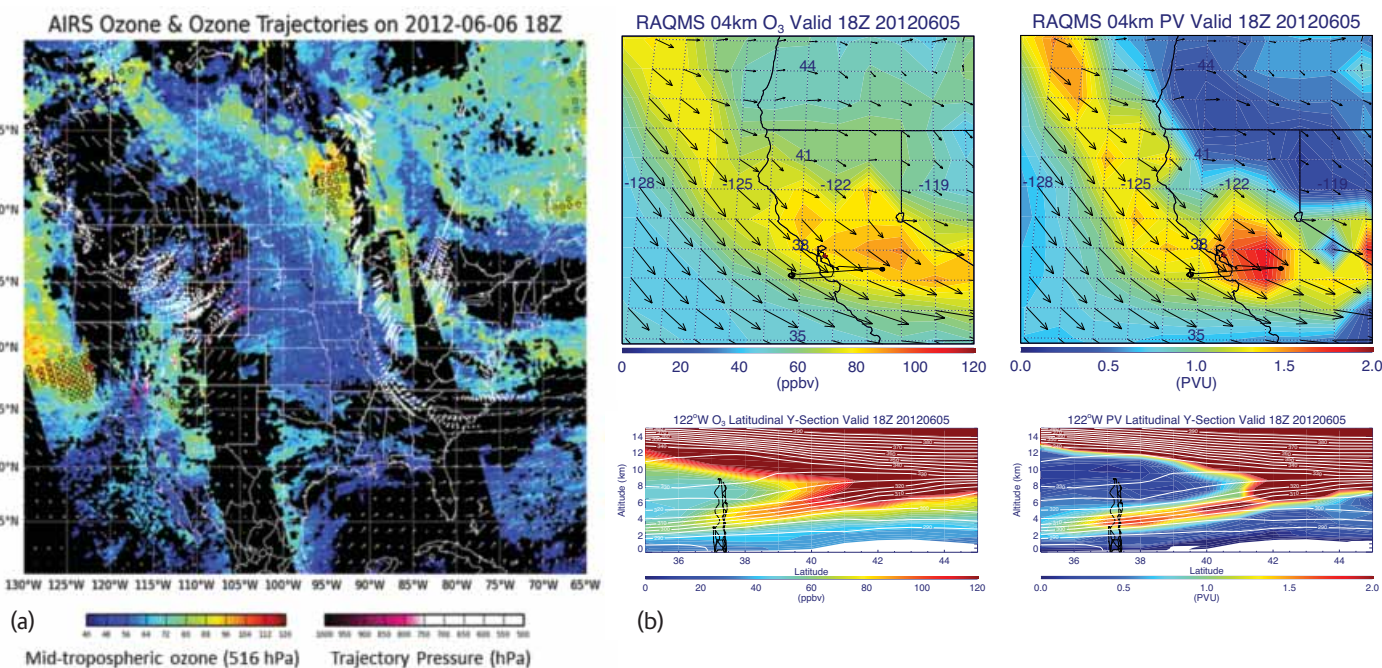


Figure 4a. IDEA-I SI forecast (magenta and white trajectories over Wyoming, Idaho, and Montana) valid at 18Z (11:00 a.m. MST) on June 6, 2012, initialized with mid-tropospheric O₃ measured by the Atmospheric Infrared Sounder (AIRS) instrument aboard the Aqua satellite on June 4, 2012. The IDEA-I SI trajectories are initialized in regions of high O₃ (open circles) off the coast of California and show the downward transport (magenta indicates high trajectory pressures near the surface) of the high O₃ air over northeastern Wyoming and Montana. The initial mid-tropospheric O₃ (516 hPa) observed with the AIRS instrument is also shown (blue-to-red color scale) along with mid-tropospheric winds (500 hPa; white arrows) from the NOAA Global Forecasting System (GFS), which are used to predict the trajectory movement. Note that the AIRS data indicate high O₃ over Canada (north of Minnesota) and trajectories were initialized there, but they never made it into the boundary layer (white trajectories over Tennessee and South Carolina).

Figure 4b. Maps at 4 km altitude (top) with wind vectors (black arrows) and cross sections at 120° W (bottom) of O₃ (ppb, left) and potential vorticity (PV; PVU, right) on June 5, 2012, at 1800 UTC from the Real-time Air Quality Modeling System (RAQMS) analyses.⁷ RAQMS stratospheric O₃ analyses are constrained through assimilation of near-real-time (NRT) O₃ profiles from satellite instruments: the Microwave Limb Sounder (MLS)¹⁶ above 50 hPa and NRT cloud cleared total column O₃ from the Ozone Monitoring Instrument (OMI),¹⁷ both aboard the Aura satellite. Also shown is the AJAX flight track (black; measurements shown in Figure 4c). Note: the tropopause fold indicated by the tongue of relatively strong PV and high O₃ extending from the lower stratosphere into the mid-troposphere (lower panels). Reproduced from Ref⁸.

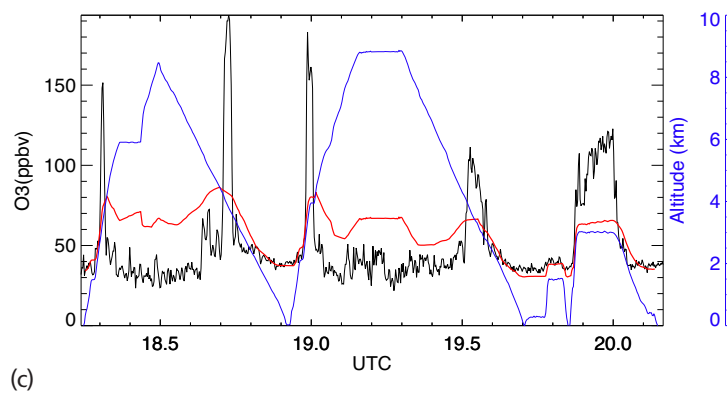


Figure 4c. Time series of observed in situ (black) and RAQMS analyzed (red; see Figure 4b) O₃ (ppb) along part of the Alpha Jet Atmospheric eXperiment (AJAX) Flight 47 track on June 5 2012. The altitude (km) of the aircraft is shown in blue. Reproduced from Ref⁸.

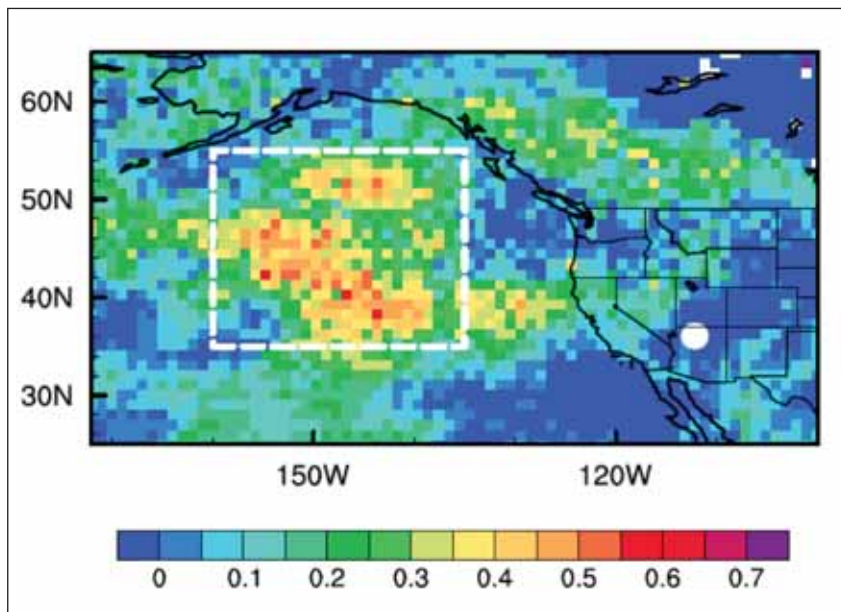


Figure 5. Correlation coefficients (r) at each $1^\circ \times 1^\circ$ grid box of May–June 2010 daily CO columns measured by the AIRS instrument on the Aqua satellite and model (AM3) estimated Asian anthropogenic enhancements to daily maximum 8-hour average O_3 at Grand Canyon National Park (white filled circle), Arizona, with a two-day time lag. The rectangle indicates the region where AIRS CO can be used to derive a space-spaced indicator of Asian influence on surface O_3 in the western U.S. Asian O_3 pollution is estimated as the difference between a standard AM3 model simulation and one with Asian anthropogenic emissions set to zero. Adapted from Ref¹⁰.

Summary

The examples above from NASA AQAQST members combine in situ and remotely sensed data with numerical simulations to attribute O_3 events measured at ground monitoring sites to three specific sources of background O_3 : wildfires, stratospheric intrusions, and Asian pollution. Air agencies can use these integrated analyses to support “exceptional event” claims for situations where multiple lines of evidence indicate that the event would not have occurred but for the influence of sources outside of their control. NASA AQAQST is working to make these tools and analysis techniques publicly available. **em**

References

1. National Ambient Air Quality Standards for Ozone; *Federal Register*, January 19, 2010; pp 2938-3052.
2. (a) Taubman, B.F.; Marufu, L.T.; Vant-Hull, B.L.; Piety, C.A.; Doddridge, B.G.; Dickerson, R.R.; Li, Z.Q. Smoke over haze: Aircraft observations of chemical and optical properties and the effects on heating rates and stability; *J. Geophys. Res.-Atmos.* **2004**, *109* (D2); (b) Colarco, P.R.; Schoeberl, M.R.; Doddridge, B.G.; Marufu, L.T.; Torres, O.; Welton, E.J. Transport of smoke from Canadian forest fires to the surface near Washington, D.C.: Injection height, entrainment, and optical properties; *J. Geophys. Res.-Atmos.* **2004**, *109* (D6), D06203.
3. (a) Singh, H.B.; Anderson, B.E.; Brune, W.H.; Cai, C.; Cohen, R.C.; Crawford, J.H.; Cubison, M.J.; Czech, E.P.; Emmons, L.; Fuelberg, H.E.; Huey, G.; Jacob, D.J.; Jimenez, J.L.; Kaduwela, A.; Kondo, Y.; Mao, J.; Olson, J.R.; Sachse, G.W.; Vay, S.A.; Weinheimer, A.; Wennberg, P.O.; Wisthaler, A. Pollution influences on atmospheric composition and chemistry at high northern latitudes: Boreal and California forest fire emissions; *Atmos. Environ.* **2010**, *44* (36), 4553-4564; (b) Singh, H.B.; Cai, C.; Kaduwela, A.; Weinheimer, A.; Wisthaler, A. Interactions of fire emissions and urban pollution over California: Ozone formation and air quality simulations; *Atmos. Environ.* **2012**, *56*, 45-51; (c) Jaffe, D.A.; Wigger, N.L. Ozone production from wildfires: A critical review; *Atmos. Environ.* **2012**, *51* (0), 1-10.
4. Lin, M.; Fiore, A.M.; Cooper, O.R.; Horowitz, L.W.; Langford, A.O.; Levy, H.; Johnson, B.J.; Naik, V.; Oltmans, S.J.; Senff, C.J. Springtime high surface ozone events over the western United States: Quantifying the role of stratospheric intrusions; *J. Geophys. Res.-Atmos.* **2012**, *117* (D21), D00V22.
5. Donner, L.J.; Wyman, B.L.; Hemler, R.S.; Horowitz, L.W.; Ming, Y.; Zhao, M.; Golaz, J.-C.; Ginoux, P.; Lin, S.J.; Schwarzkopf, M.D.; Austin, J.; Alaka, G.; Cooke, W.F.; Delworth, T.L.; Freidenreich, S.M.; Gordon, C.T.; Griffies, S.M.; Held, I.M.; Hurlin, W.J.; Klein, S.A.; Knutson, T.R.; Langenhorst, A.R.; Lee, H.-C.; Lin, Y.; Magi, B.I.; Malyshev, S.L.; Milly, P.C.D.; Naik, V.; Nath, M.J.; Pincus, R.; Ploshay, J.J.; Ramaswamy, V.; Seman, C.J.; Sheviakova, E.; Sirtus, J.J.; Stern, W.F.; Stouffer, R.J.; Wilson, R.J.; Winton, M.; Wittenberg, A.T.; Zeng, F. The Dynamical Core, Physical Parameterizations, and Basic Simulation Characteristics of the Atmospheric Component AM3 of the GFDL Global Coupled Model CM3; *J. Climate* **2011**, *24* (13), 3484-3519.
6. Al-Saadi, J.; Szykman, J.; Pierce, R.B.; Kittaka, C.; Neil, D.; Chu, D.A.; Remer, L.; Gumley, L.; Prins, E.; Weinstock, L.; MacDonald, C.; Wayland, R.; Dimmick, F.; Fishman, J. Improving National Air Quality Forecasts with Satellite Aerosol Observations; *Bull. Am. Meteorol. Soc.* **2005**, *86* (9), 1249-1261.
7. Pierce, R.B.; Schaack, T.; Al-Saadi, J.A.; Fairlie, T.D.; Kittaka, C.; Lingenfelter, G.; Natarajan, M.; Olson, J.; Soja, A.; Zapotocny, T.; Lenzen, A.; Stobie, J.; Johnson, D.; Avery, M. A.; Sachse, G.W.; Thompson, A.; Cohen, R.; Dibb, J.E.; Crawford, J.; Rault, D.; Martin, R.; Szykman, J.; Fishman, J. Chemical data assimilation estimates of continental U.S. ozone and nitrogen budgets during the Intercontinental Chemical Transport Experiment–North America; *J. Geophys. Res.-Atmos.* **2007**, *112* (D12), D12S21.
8. Yates, E. L.; Iraci, L. T.; Roby, M. C.; Pierce, R. B.; Johnson, M. S.; Reddy, P. J.; Tadjifá, J. M.; Loewenstein, M.; Gore, W., Airborne observations and modeling of springtime stratosphere-to-troposphere transport over California. *Atmos. Chem. Phys. Discuss.* **2013**, *13* (4), 10157-10192.
9. United Economic Commission for Europe (UNECE) Task Force on Hemispheric Transport of Air Pollution (TF HTAP) *HEMISPHERIC TRANSPORT OF AIR POLLUTION 2010 PART A: OZONE AND PARTICULATE MATTER*, Air Pollution Studies No. 17; UNITED NATIONS: New York, 2010.
10. Lin, M.; Fiore, A.M.; Horowitz, L.W.; Cooper, O.R.; Naik, V.; Holloway, J.; Johnson, B.J.; Middlebrook, A.M.; Oltmans, S.J.; Pollack, I.B.; Ryerson, T.B.; Warner, J.X.; Wiedinmyer, C.; Wilson, J.; Wyman, B. Transport of Asian ozone pollution into surface air over the western United States in spring. *J. Geophys. Res.* **2012**, *117*, D00V07.
11. *Integrated Science Assessment of Ozone and Related Photochemical Oxidants (Final Report)*; U.S. Environmental Protection Agency, Washington, DC, 2013.
12. *Global Sources of Local Pollution: An Assessment of Long-Range Transport of Key Air Pollutants to and from the United States*; National Academy of Sciences National Research Council (NRC); The National Academies Press: Washington, DC, 2009.
13. For example: (a) Fiore, A.; Jacob, D.J.; Liu, H.; Yantosca, R.M.; Fairlie, T.D.; Li, Q. Variability in surface ozone background over the United States: Implications for air quality policy. *J. Geophys. Res.* **2003**, *108* (D24), 4787; (b) Zhang, L.; Jacob, D.J.; Downey, N.V.; Wood, D.A.; Blewitt, D.; Carouge, C.C.; van Donkelaar, A.; Jones, D.B.A.; Murray, L.T.; Wang, Y. Improved estimate of the policy-relevant background ozone in the United States using the GEOS-Chem global model with $1/2^\circ \times 2/3^\circ$ horizontal resolution over North America; *Atmos. Environ.* **2011**, *45* (37), 6769-6776.
14. (a) Mueller, S.F.; Mallard, J.W. Contributions of Natural Emissions to Ozone and PM_{2.5} as Simulated by the Community Multiscale Air Quality (CMAQ) Model; *Environ. Sci. Technol.* **2011**, *45* (11), 4817-4823; (b) McKeen, S.A.; Wotawa, G.; Parrish, D.D.; Holloway, J.S.; Buhr, M.P.; Hübler, G.; Fehsenfeld, F.C.; Meagher, J.F. Ozone production from Canadian wildfires during June and July of 1995; *J. Geophys. Res.-Atmos.* **2002**, *107* (D14), ACH 7-1-ACH 7-25; (c) Emery, C.; Jung, J.; Downey, N.; Johnson, J.; Jimenez, M.; Yarwood, G.; Morris, R. Regional and global modeling estimates of policy relevant background ozone over the United States; *Atmos. Environ.* **2012**, *47* (0), 206-217.
15. Yienger, J.J.; Galanter, M.; Holloway, T.A.; Phadnis, M.J.; Guttikunda, S.K.; Carmichael, G.R.; Moxim, W.J.; Levy, H., II The episodic nature of air pollution transport from Asia to North America; *J. Geophys. Res.* **2000**, *105* (D22), 26931-26945.
16. Waters, J.W.; Froidevaux, L.; Harwood, R.S.; Jarnot, R.F.; Pickett, H.M.; Read, W.G.; Siegel, P.H.; Cofield, R.E.; Filipiak, M.J.; Flower, D.A.; Holden, J.R.; Lau, G.K.; Livesey, N.J.; Manney, G.L.; Pumphrey, H.C.; Santee, M.L.; Wu, D.L.; Cuddy, D.T.; Lay, R.R.; Loo, M.S.; Perun, V.S.; Schwartz, M.J.; Stek, P.C.; Thurstant, R.P.; Boyles, M.A.; Chandra, K.M.; Chavez, M.C.; Gun-Shing, C.; Chudasama, B.V.; Dodge, R.; Fuller, R.A.; Girard, M.A.; Jiang, J.H.; Yibo, J.; Knosp, B.W.; LaBelle, R.C.; Lam, J.C.; Lee, K.A.; Miller, D.; Oswald, J.E.; Patel, N.C.; Pukala, D.M.; Quintero, O.; Scaff, D.M.; Van Snyder, W.; Tope, M.C.; Wagner, P.A.; Walch, M.J. The Earth observing system microwave limb sounder (EOS MLS) on the aura Satellite; *Geoscience and Remote Sensing, IEEE Transactions* **2006**, *44* (5), 1075-1092.
17. Levelt, P.F.; Van den Oord, G.H.J.; Dobber, M.R.; Malkki, A.; Huib, V.; de Vries, J.; Stammes, P.; Lundell, J.O.V.; Saari, H. The ozone monitoring instrument. *Geoscience and Remote Sensing, IEEE Transactions* **2006**, *44* (5), 1093-1101.